UDC 669 . 14 . 018 . 8 : 669 . 74

Technical Report

Development of NSSC® 304JS, Ultra-soft Austenitic Stainless Steel with Excellent Formability

Masaharu HATANO* Akihiko TAKAHASHI

Abstract

Herein described are the basic philosophy for the chemical design to realize good formability for a new stainless steel, NSSC 304JS, as well as the properties and applications of commercially produced sheets of the developed steel. The effects of adding Mn on work-induced structure were examined and effectively utilized to obtain good secondary working properties. The developed steel is characterized by its ultra-soft texture, formability and magnetizing properties that greatly exceed those of conventional JIS SUS304 and SUS304J1L, making it more suitable for applications where secondary working or multistage drawing is required. Thanks to its excellent formability, NSSC 304JS has been used for heavy forming applications such as automobile parts, kitchen facilities and electrical appliances.

1. Introduction

Metastable austenitic (γ) stainless steels[1], typically such as JIS SUS304 and SUS304J1L, are used for a wide variety of applications by virtue of their well-balanced corrosion resistance and formability. Although these steels exhibit high ductility and stretchability because of the formation of strain-induced α' martensite, their deep-drawability and secondary working properties are not as good.

Various new methods of forming stainless steel sheets have been introduced in recent years, but in some cases, the conditions during secondary work or deep drawing are too demanding for metastable austenitic stainless steels. For example, in the case of multistage drawing or that of spinning, stretching or other secondary working after deep drawing, it is essential to soften the material, suppress work hardening, and control work-induced structure to give it properties suitable for secondary working. To soften the material and minimize work hardening, it is necessary to use innovative smelting technologies to decrease the contents of elements (C, N, etc.) that strengthen austenite (γ) by solid solution hardening, and to enhance the stability of austenite and thus minimize the formation of strain-induced α' martensite. In view of this, the authors examined the effects of austenite-forming elements, Mn, Cu and Ni, on the secondary working properties of ultra-soft, ultra-low-C, ultra-low-N, austenitic stainless steel from resource-saving and economical viewpoints, focusing especially on the effective use of Mn.

Based on the above concepts, by controlling the amounts of Mn, Cu and Ni added and through optimal combination of the formation of strain-induced α' martensite and the work hardening of austenite (γ) to maximize secondary working properties, Nippon Steel & Sumikin Stainless Steel Corporation developed ultra-soft, high-formability austenitic stainless steel, NSSC® 304JS. This paper explains the philosophy for the material design of the developed steel, the design details of the steel chemistry to optimize secondary working properties, the mechanical and other properties of commercially produced NSSC 304JS, and its applications.

2. Philosophy of Material Design

Fig. 1 schematically explains the chemical design of NSSC 304JS in terms of C and N contents and Md_{30} in comparison with conventional stainless steels. Md_{30} is widely known as an index to show the ease with which strain-induced α' martensite forms[1]; the empirical formula shown below was used in the present study[2]. Austenite (γ)

NSSC® is a registered trademark of Nippon Steel & Sumikin Stainless Steel Corporation.

* Senior Researcher, D. Eng., Research & Development Center, Nippon Steel & Sumikin Stainless Steel Corporation
3434, Ooaza-shimata, Hikari, Yamaguchi

becomes more stable and the formation of strain-induced α' martensite more difficult, as the value of Md_{30} becomes smaller.

$$Md_{30}\ (℃) = 551 - 462\ (C + N) - 9.2\ (Si) - 8.1\ (Mn) - 13.7\ (Cr) - 29\ (Ni + Cu) - 18.2\ (Mo)$$

(contents in mass %)

SUS304 (18Cr-8Ni steel for general use), 18Cr-9Ni steel (a variation of SUS304 for deep-drawing use) and SUSXM7 (9Ni-3Cu steel) have total C and N contents decreasing in that order, and their Md_{30} values also decrease in the same order, with increasing content of such austenite-forming elements as Ni and Cu. In order to soften NSSC 304JS, an innovative smelting process was introduced to decrease the total content of C and N to a very low level. The chemical composition of NSSC 304JS was defined based on that of SUS304J1L, a low-Ni, metastable austenitic steel containing Cu, and to suppress the formation of strain-induced α' martensite, the Mn content was increased to set the value of Md_{30} at the same level as that of 18Cr-9Ni steel. The targets in the above chemical design of NSSC 304JS were to soften the material and improve general formability by decreasing total C and N content to below that of conventional steels[3, 4], and to improve deep drawability by effective use of Mn to stabilize austenite (γ).

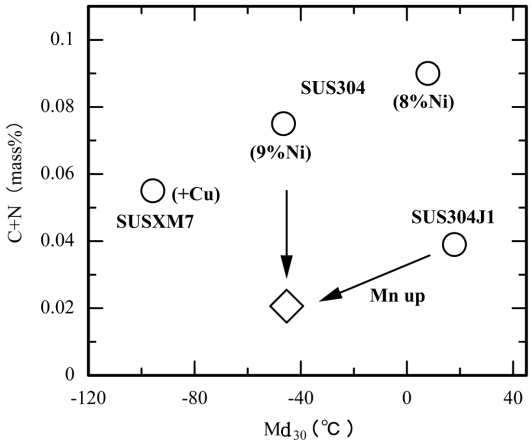

Fig. 1 Basic concept for chemical design of NSSC 304JS

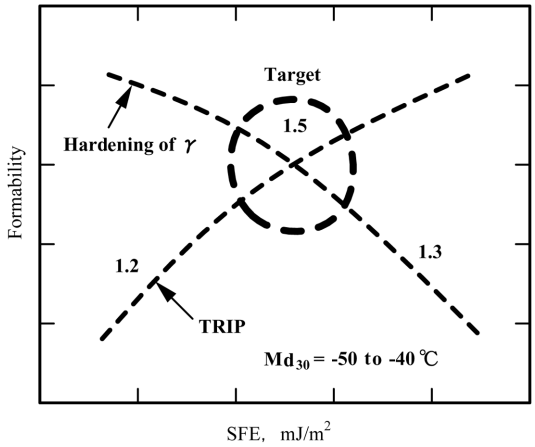

Fig. 2 Philosophy for improvement of secondary working properties and control of work-induced structure (1.2, 1.3, 1.5: stretch-flanging ratios after 40% cold rolling)

Fig. 2 schematically shows the philosophy for improvement of secondary working properties and control of work-induced structure. Secondary working properties are determined, among other factors, by transformation-induced plasticity (TRIP) due to the formation of strain-induced α' martensite and by work hardening of austenite (γ). So as to show the effects of TRIP and work hardening of austenite (γ) schematically, the graph plots stacking fault energy (SFE) along the horizontal axis. Figures 1.2, 1.3 and 1.5 present the stretch flanging ratios after 40 percent cold rolling, the ratio which is used as an indicator of secondary working properties. A steel chemistry to optimize secondary working properties (or stretch flanging ratio) through combination of TRIP and work hardening of austenite (γ) was conceived as shown by the dotted circle in the graph[5, 6]. The alloy design will be explained in more detail in Section 4.

3. Test Methods

In the first place, the authors conducted various tests to define an alloy design that would bring about excellent secondary working properties. The methods of the tests are described below.

Specimen ingots of an ultra-low-C, ultra-low-N, 17Cr steel having different contents of Mn, Cu and Ni in the respective ranges shown in **Table 1** were prepared through vacuum refining. The ingots were hot rolled into plates 5 mm in thickness, annealed at 1050℃ for 60 s, cold rolled to a thickness of 1.5 mm, annealed at 1000℃ for 60 s, and then subjected to Vickers hardness measurement and evaluation tests of secondary working properties. The cold-rolled and annealed sheets were cold rolled again at 40 percent reduction, a 10-mm hole was drilled in each specimen sheet by machining, the hole was expanded using a punch with a head angle of 60° until its edge fractured (hole-expanding test), and the secondary working properties were evaluated in terms of the ratio of increase in the hole diameter before and after the hole-expanding work (stretch flanging ratio λ). The amount of the α' phase was measured using a ferrite meter made by Fischer, and the work-induced structure was observed through a transmission electron microscope (TEM) using thin-film samples taken from the specimens after the hole-expanding test.

Next, NSSC 304JS was manufactured on commercial production facilities based on the above study results, and the properties of the product were evaluated in the following manner. Mechanical properties were tested through tensile tests using JIS No. 13 B test pieces, and workability through the Erichsen test under JIS Z 2247 and pressure bulge tests. Deep drawability in multistage drawing was evaluated in terms of the drawing ratio at which delayed cracking occurred (limit drawing ratio - LDR) in seven-stage cup drawing test using initial blanks 96 mm in diameter and punches 22, 25, 30, 35, 40, 44 and 48 mm in diameter. With respect to square drawability, square-drawing tests were conducted using initial blanks 220 mm square and a punch 103 mm square at a blank holding force of 40 t, and sheet thickness distribution and magnetization were evaluated

Table 1 Chemical compositions of specimens (mass%)

C	Si	Mn	Ni	Cu	Cr	N	Md_{30}
0.005 - 0.010	0.35 - 0.45	1.4 - 4.4	7.0 - 9.5	1.6 - 4.0	17.0 - 17.7	0.010 - 0.014	–15.0 - –50.0

$Md_{30}\ (℃) = 551 - 462\ (C + N) - 9.2Si - 8.1Mn - 13.7Cr - 29\ (Ni + Cu) - 18.2Mo$

in comparison with conventional austenitic steels. Here, magnetization was evaluated by measuring the amount of the α' phase after square drawing using a ferrite meter made by Fischer. Corrosion resistance was evaluated by measuring pitting potential according to JIS Z 0577 under conditions of temperature changes from 20℃ to 80℃ and Cl^- concentration from 20 ppm to 20,000 ppm.

4. Test Results and Discussion

The results of the alloy design to achieve good secondary working properties are explained here in detail.

Fig. 3 shows the relationship between Md_{30} and stretch flanging ratio (λ), an indicator of secondary working properties. The white and black circles represent steel specimens with different Mn contents as described beneath the caption of **Fig. 4**. Because the Cu content is different between the white circles and the black circle, the Md_{30} values are different even when the Mn content is the same. The hardness of all the specimens was controlled to approximately HV 130. Looking at the curve of the white circles of the graph, as Md_{30} decreases, the stretch-flanging ratio (λ) increases to hit a maximum value when Md_{30} takes a specific value in the range from –20℃ to –40℃. This behavior of λ is similar to what has been reported in past papers[4, 7]. It is worth noticing here that the values of λ for the white and black circles near the Md_{30} value of –30℃ differ greatly from each other. This indicates that work-induced structure, which changes depending on alloy contents, affects secondary working properties as a third factor in addition to Md_{30} and material hardness.

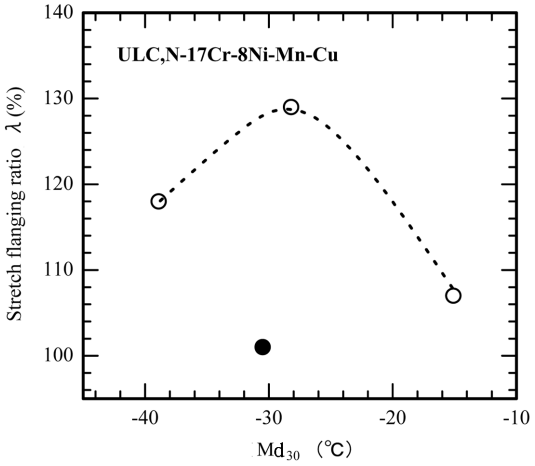

Fig. 3 Relationship between stretch-flanging ratio after 40% cold rolling and Md_{30} (indicater for stability of γ phase)

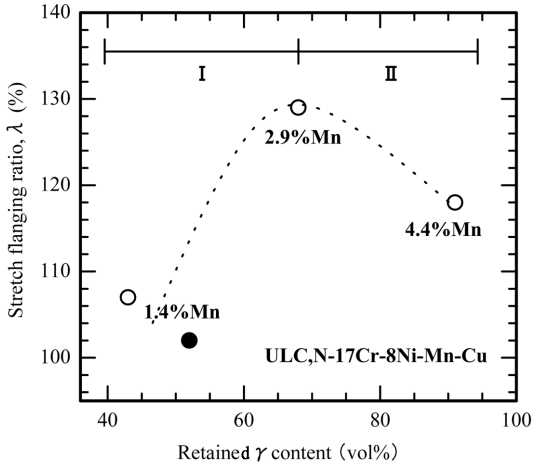

Fig. 4 Relationship between stretch-flanging ratio and amount of retained austenite
Md_{30} (℃), ○ : 1.4%Mn = –15, 2.9%Mn = –28, 4.4%Mn = –38
Md_{30} (℃), ● : 1.4%Mn = –31

Fig. 4 shows the above test result with respect to the amount of retained austenite (γ); here the amount of retained austenite was calculated by subtracting the percentage volume of martensite α' measured near the fracture of the hole expanding from 100 percent. The amount of austenite retained increases with increasing Mn content, and λ peaks at a certain amount of retained austenite. Focusing attention on the region where Md_{30} is roughly –30℃, it is notable that the amount of retained austenite (γ) and λ increase as the Mn content increases (black circle: 1.4% Mn, white circle: 2.9% Mn). This indicates that the addition of Mn is effective in suppressing the formation of work-induced martensite (α') after 40 percent cold reduction and thus increases the stretch-flanging ratio λ (see Region I in Fig. 4), more effectively than it appears to be in the formula of Md_{30} given in Section 2.

One can understand from Fig. 4 that λ increases in proportion to the amount of retained austenite (γ) when the latter amount is from 44 to 77 percent. This indicates that, as far as ultra-low-C, ultra-low-N, austenitic stainless steels are concerned, the contribution of retained austenite (γ) to the increase of λ is significant. In view of this, in addition to the TRIP due to the formation of work-induced martensite (α'), the authors included the work-hardenability of retained austenite as a factor to influence λ , thus:

$$\lambda = X + Y, \quad (1)$$

where, X is the influence of TRIP due to the formation of work-induced martensite (α'), and Y is that of the work hardening of retained austenite (γ).

Then, using regression analysis and assuming that Equation (1) held true, the coefficients for alloy elements corresponding to parameters X and Y were calculated from the test results of specimen steels containing Mn, Cu and Ni using different amounts in the ranges shown in Table 1. The analysis results are shown in the equation below and **Fig. 5**[8].

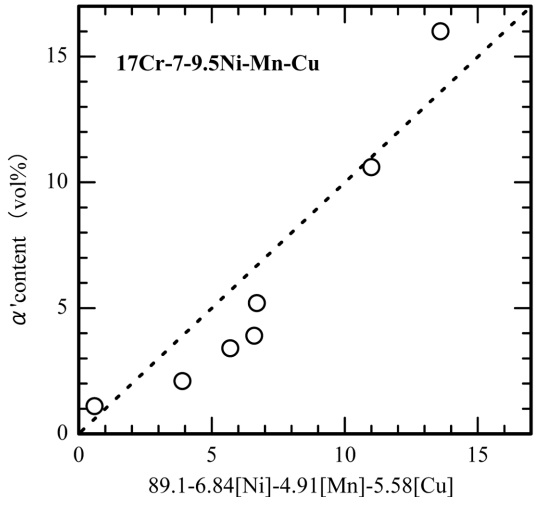

Fig. 5 Effects of Ni, Mn, Cu on stretch flanging ratio after 40% cold rolling
A = 13.3 – (Mn + Ni + 0.72Cu), B = Mn + 0.91Ni – 0.78Cu (mass%)

$$\lambda\ (\%) = 14.1A + 15.0B - 23.5 \quad (2)$$
$$A = 13.3 - (Mn + Ni + 0.72Cu) \quad (\text{in mass } \%)$$
$$B = Mn + 0.91Ni + 0.78Cu \quad (\text{same})$$

In Equation (2), the term 14.1A represents the amount of work-induced martensite (α '), and Mn, Cu and Ni, which help the formation of retained austenite (γ) and suppress that of work-induced martensite (α '), have negative coefficients. On the other hand, the term 15.0B corresponds to the work-hardenability of retained austenite (γ). Mn and Ni, which have positive coefficients in the second equation below Equation (2), are considered to accelerate the work hardening of retained austenite (γ) near the fracture during hole-expanding work, and Cu, which has a negative coefficient, to hinder the work hardening. Here, while Ni is a major constituent element (7 percent or more) of the developed steel following Cr, the authors focused attention rather on the difference in the effects of Mn and Cu. That is to say, the analysis results indicate that, in a high-strain region where secondary working properties show, Mn decreases stacking fault energy causing the work-hardenability of retained austenite (γ) to increase, while Cu has the inverse effect. In fact, E. B. Pickering reported the effect of Mn lowering the stacking fault energy[9], and D. Dulieu et al. the effects of Cu to increase it[10].

Based on the above result, the authors assumed that the increase in stretch flanging ratio (λ) in Region I of Fig. 4 resulted from an increase in the work-hardenability of retained austenite (γ) due to Mn addition, and the decrease in λ in Region II of the graph, from the decrease in the amount of work-induced martensite (α '), or the decrease in TRIP.

Looking for structural features evidencing the decrease in stacking fault energy in a high-strain region due to Mn addition mentioned earlier, the authors observed work-induced structure through a TEM. **Fig. 6** shows TEM images of thin-film specimens taken from the vicinity of the fracture at the hole-expanding test of the 1.4- and 2.9-percent Mn steels shown in Fig. 4. Whereas the 1.4-percent Mn specimen (a) had cellular structures where dislocations are unevenly and irregularly distributed, the 2.9-percent Mn specimen (b) demonstrated characteristic band structures (indicated with arrows) in addition to similar cellular structures. The authors confirmed later that the band structures resulted from austenite (γ) twins. It has been known that work-induced structure of austenite (γ) is likely to have dislocations in planar arrangements because of a decrease in stacking fault energy[11], and consequently, austenite twins easily form[12]. It follows, therefore, that the observed change in work-induced structure occurred presumably because of a decrease in stacking fault energy due to Mn addition. In other words, the authors consider that the increase in the work-hardenability of retained austenite due to Mn addition resulted from austenite twins that form in a high-strain region.

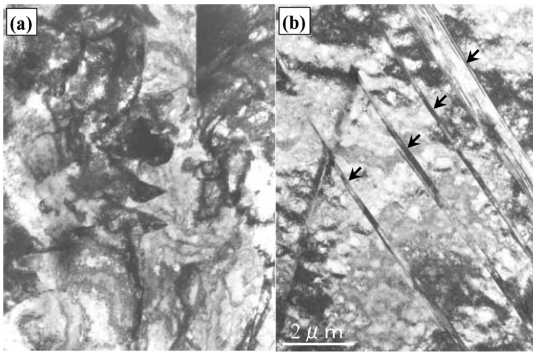

Fig. 6 Bright-field TEM images of (a) 1.4%Mn and (b) 2.9%Mn steel shown in Fig. 4
(Thin foil specimens were taken from near the fractures of the test pieces ahter 40% cold rolling and hole expanding.)

5. Characteristics of NSSC 304JS

This section explains the characteristic properties of commercially manufactured NSSC 304JS, the chemistry of which was designed based on the detailed examinations described above.

A typical example of the chemical composition of NSSC 304JS is shown in **Table 2**. The steel chemistry is principally based on that of a 17%Cr-8%Ni steel, but the contents of C, N and other impurity elements are decreased to the lowest possible level, and Mn and Cu are added to soften the material and improve secondary working properties. **Table 3** compares the mechanical properties of cold-rolled sheets of NSSC 304JS (test piece thickness: 1.5 mm) with those of SUS304. The 0.2-percent proof stress of NSSC 304JS is roughly 200 N/mm^2, its tensile strength roughly 490 N/mm^2, and the hardness HV 109, considerably lower (softer) than those of SUS304, while its elongation is the same.

The evaluation of the workability of the developed steel is explained hereunder according to the test methods described in Section 3. Note that cold-rolled sheets of 2D finish and 1.5-mm thick were used for the hole-expanding test, and those of 2B finish 0.8-mm thick for the press-forming test.

Fig. 7 shows the results of hole-expanding (stretch-flanging) test of cold-rolled sheets. The developed steel showed a very high stretch-

Table 2 Chemical composition of NSSC 304JS (mass%)

C	Si	Mn	Ni	Cu	Cr	N
0.009	0.46	2.7	8.0	2.7	17.4	0.011

Table 3 Mechanical properties of NSSC 304JS and SUS304 steel sheets

	0.2%PS (N/mm^2)	TS (N/mm^2)	EL (%)	Hv (49N)
NSSC 304JS	201	492	59	109
SUS304	274	680	59	170

JIS products, 2D finish

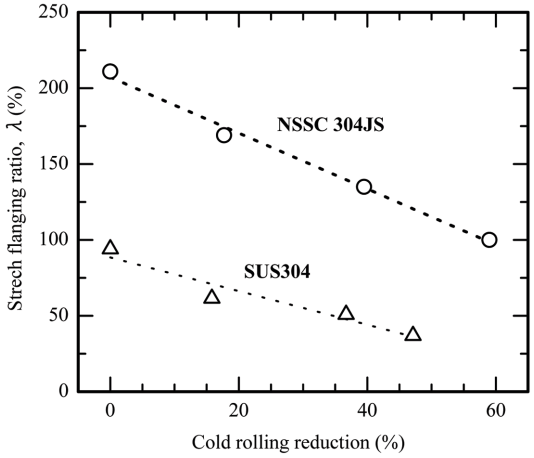

Fig. 7 Stretch flanging ratio after cold rolling of NSSC 304JS and SUS304 steel sheets

flanging ratio, twice that of SUS304 or higher after cold rolling at different reduction ratios, evidencing excellent secondary working properties as envisaged in the development.

Table 4 compares NSSC 304JS with SUS304 in terms of typical indicators of formability. The n-value of NSSC 304JS is sufficiently low compared with that of SUS304, which indicates that work hardening is effectively suppressed. With respect to pressure bulging height, an indicator of pure stretch formability, on the other hand, the result of NSSC 304JS was higher than that of SUS304, reflecting the material softness and high elongation.

Table 5 shows a comparison of deep drawability at the multistage drawing test, and **Fig. 8** the appearances of specimens after the test. Whereas delayed cracking occurred with SUS304 after the third stage to a total drawing ratio of 2.4, no such cracking occurred with the developed steel even after seven-stage drawing to a total drawing ratio of 4.4, evidencing excellent resistance to delayed cracking. The significant improvement in deep drawability in multistage drawing is due to the softening of the steel material and the stabilization of the γ phase through Mn addition.

Fig. 9 shows the sheet thickness change in square drawing and the appearance of a specimen; the sheet thickness was measured from A to B as indicated by the arrow in the photograph. The ratio of thickness change was calculated by dividing the thickness after the drawing t by the thickness before t_0. As is clear from the graph, the thickness change of the developed steel was smaller than that of SUS304, which means that its plastic deformation during forming work is more homogeneous. **Fig. 10** shows the amount of work-induced martensite (α ') measured along the same line after the square drawing; the α ' phase is magnetic and the γ phase non-magnetic. The graph shows that NSSC 304JS exhibits far lower magnetism after forming work than SUS304 does.

Fig. 11 shows pitting potential under different conditions of temperature and Cl^- concentration. The curves indicate the points where pitting potential V_C' 100 (Vv.s.AgCl) is 0.2 V under the measurement conditions. The value 0.2 V is considered the potential at which stainless steel is prevented from rusting by washing with water[1], and thus corrosion is likely to occur in the region above the curves. The graph includes also the curves for SUS304, SUS304J1L and SUS430. The pitting-corrosion resistance of the developed steel is equal to that of SUS304 except when salinity is equal to or higher than that of seawater, and is superior to that of SUS304J1L.

As explained herein, NSSC 304JS is an ultra-soft steel, has excellent formability, and as such, is suitable for applications requiring

Table 4 Formability of NSSC 304JS and SUS304 steel sheets

	n-value	r-value	Erichsen height (mm)	Bulge height (mm)
NSSC 304JS	0.39	0.98	13.5	42.2
SUS304	0.49	0.97	13.4	40.3

JIS products, 2B finish

Table 5 Deep drawability in multistage drawing of NSSC 304JS and SUS304 steel sheets

Punch (mm)	48	44	40	35	30	25	22
Die (mm)	51	47	43	38	33	28	25
L.D.R.	2.0	2.2	2.4	2.7	3.2	3.8	4.4
NSSC 304JS	○	○	○	○	○	○	○
SUS304	○	○	▲				

○ : No cracking ▲ : Delayed cracking
JIS products, 2B finish

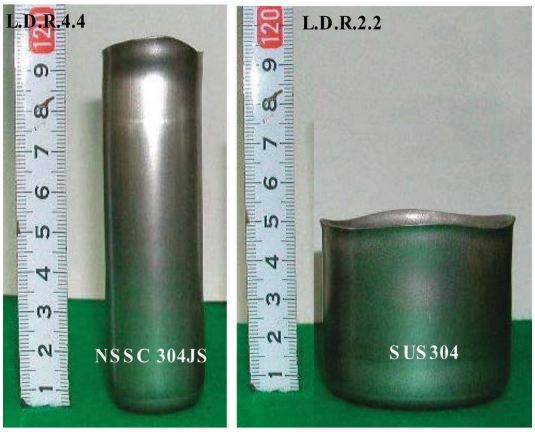

Fig. 8 Appearances of specimens after multistage drawing test

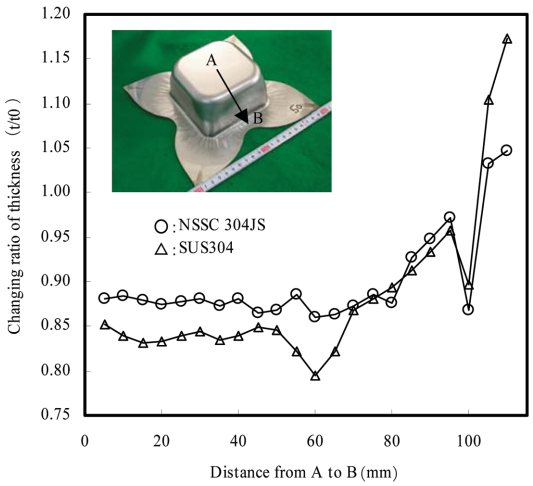

Fig. 9 Thickness change after square drawing of NSSC 304JS and SUS304 steel sheets

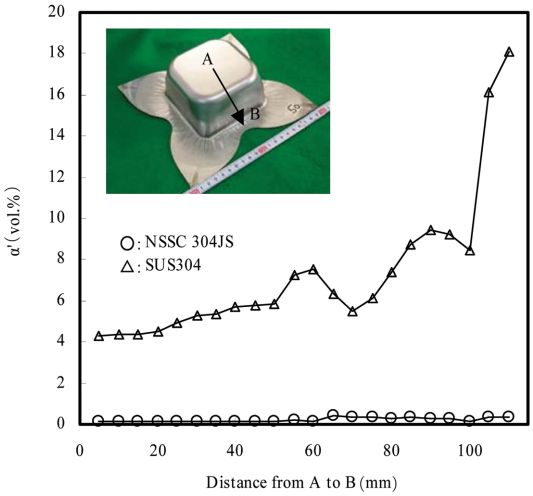

Fig. 10 Amount of α ' phase induced by square-deep drawing of NSSC 304JS and SUS304 steel sheets

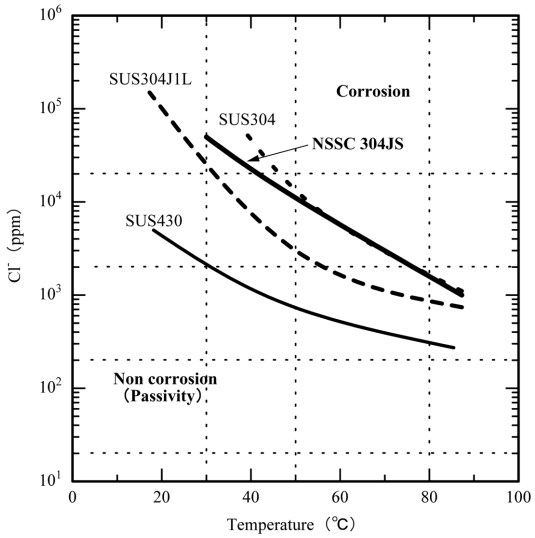

Fig. 11 Pitting potential of 0.2V (Vv.s.AgCl) underdifferent conditions of Cl^- concentration and temperature

secondary working, multistage drawing and other press forming work into complicated shapes. It is also suitable for those applications where low polarization after forming work is desirable. The workability of the developed steel can be further enhanced by applying lubricating coating[5]. Thanks to these advantages, NSSC 304JS has been used for a wide variety of applications such as automobile parts and kitchen facilities that require high formability, and electric appliances where low polarization after forming work is desirable.

6. Closing

This paper has explained the basic philosophy for the material design of NSSC 304JS, detailed studies of its alloy design to achieve good secondary working properties, the characteristics of commercially manufactured sheet products, and actual applications.

The alloy design of NSSC 304JS is characterized by maximization of secondary working properties taking advantage of the effects of Mn that show in a high-strain region, and combining the formation of strain-induced α' martensite and the work hardening of retained austenite (γ). In consideration of its softness, high workability and low magnetization after forming work, use of the developed steel is expected to expand to cover a wide variety of applications.

References

1) Japan Stainless Steel Association: Stainless Steel Handbook. 3rd Edition. The Nikkan Kogyo Shimbun, Ltd., Tokyo, 1995, 554p
2) Nohara, K., Ono, H., Ohashi, N.: Tetsu-to-Hagané. 63, 772 (1977)
3) Arakawa, M., Sumitomo, H.: Tetsu-to-Hagané. 65, 472 (1979)
4) Itoh, N., Ogaya, M., Yokoyama, K., Ishiyama, S.: Nippon Stainless Technical Report. 13, 1 (1977)
5) Hatano, M. et al.: CAMP-ISIJ. 17 (3), 410 (2004)
6) Takahashi, A., Hatano, M., Kimura, K.: Journal of the Japan Society for Technology of Plasticity. 46 (530), 194 (2005)
7) Suzuki, S., Tanaka, H., Miyakusu, K.: CAMP-ISIJ. 13 (3), 552 (2000)
8) Hatano, M., Takahashi, A.: CAMP-ISIJ. 19 (6), 1163 (2006)
9) Pickering, E.B.: Stainless Steel '84, The Inst. of Metals, London, 1984, p. 2
10) Dulieu, D., Nutting, J.: Met.Trans. 2, 140 (1968)
11) Remy, L., Pineau, A.: Materials Science and Engineering. 28, 9 (1977)
12) Kurdjumov, G.V.: Fiz. Met Metalloved. 42, 527 (1976)

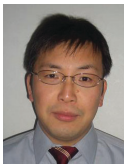

Masaharu HATANO
Senior Researcher, D. Eng.,
Research & Development Center,
Nippon Steel & Sumikin Stainless Steel Corporation
3434, Ooaza-shimata, Hikari, Yamaguchi

Akihiko TAKAHASHI
General Manager, Research & Development Center,
Nippon Steel & Sumikin Stainless Steel Corporation,
Chief Researcher, D.Eng.